Eur Radiol (2009) 19: 1799–1808
DOI 10.1007/s00330-009-1347-0

NEURO

Elke Hattingen
Richard DuMesnil
Ulrich Pilatus
Andreas Raabe
Timo Kahles
Jürgen Beck

Contrast-enhanced MR myelography in spontaneous intracranial hypotension: description of an artefact imitating CSF leakage

Received: 5 September 2008
Revised: 3 January 2009
Accepted: 12 January 2009
Published online: 24 February 2009

E. Hattingen (✉) · R. DuMesnil · U. Pilatus
Institute of Neuroradiology,
University of Frankfurt,
Schleusenweg 2 – 16,
60528 Frankfurt, Germany
e-mail: elke.hattingen@kgu.de
Tel.: +49-69-63015462
Fax: +49-69-63017176

A. Raabe · J. Beck
Department of Neurosurgery,
University of Frankfurt,
Frankfurt, Germany

T. Kahles
Department of Neurology,
University of Frankfurt,
Frankfurt, Germany

Abstract In contrast-enhanced (CE) MR myelography, hyperintense signal outside the intrathecal space in T1-weighted sequences with spectral presaturation inversion recovery (SPIR) is usually considered to be due to CSF leakage. We retrospectively investigated a hyperintense signal at the apex of the lung appearing in this sequence in patients with SIH (n=5), CSF rhinorrhoea (n=2), lumbar spine surgery (n=1) and in control subjects (n=6). Intrathecal application of contrast agent was performed in all patients before MR examination, but not in the control group. The reproducible signal increase was investigated with other fat suppression techniques and MR spectroscopy. All patients and controls showed strongly hyperintense signal at the apex of the lungs imitating CSF leakage into paraspinal tissue. This signal increase was identified as an artefact, caused by spectroscopically proven shift and broadening of water and lipid resonances (1–2 ppm) in this anatomical region. Only patients with SIH showed additional focal enhancement along the spinal nerve roots and/or in the spinal epidural space. In conclusion CE MR myelography with spectral selective fat suppression shows a reproducible cervicothoracic artefact, imitating CSF leakage. Selective water excitation technique as well as periradicular and epidural contrast collections may be helpful to discriminate between real pathological findings and artefacts.

Keywords CE MR myelography · Spontaneous intracranial hypotension · Artefact · SPIR · MR spectroscopy

Introduction

In 1938 Schaltenbrandt described a spontaneous form of intracranial hypotension which he attributed to "Aliquorrhoe" [1]. Since then several pathophysiological mechanisms of spontaneous intracranial hypotension (SIH) syndrome have been discussed [2]. Spontaneous intracranial hypotension is an increasingly recognized cause of daily orthostatic headaches, particularly among young and middle-aged individuals, but an initial misdiagnosis remains common [3]. The annual incidence of SIH is estimated at 5 per 100,000, with a female/male ratio of approximately 2:1 [3]. The International Classification of Headache Disorders consortium has recently classified the syndrome of SIH and defined diagnostic criteria. The intensity of the headache varies widely, but the pain typically improves 15–30 min after lying down. Most common distinct associated symptoms are posterior neck pain, neck stiffness, nausea and vomiting. Typical findings of cranial MRI include diffuse fine line pachymeningeal enhancement secondary to dural venous dilation, sagging of the brain with tonsillar descent, a decrease in the size of the prepontine and prechiasmatic cisterns, and inferior displacement of the optic chiasm. Other common findings include slit-like ventricles and subdural fluid collections or even subdural haematomas. Beside cranial MRI other important diagnostic criteria are the cerebrospinal fluid (CSF) opening pressure below 60 mm H_2O in the sitting

Table 1 Participants of the MR study, symptoms, treatment and follow-up

Participant	Age (years)	Sex	Symptoms	Treatment/follow-up
Pt 1	31	F	SIH	Blood patch level C7/TH1, distribution C4-TH 2; clinical improvement
Pt 2	37	F	SIH	Two sessions with blood patch level C6/7, distribution C2-TH1/2; clinical improvement after each session
Pt 3	45	M	SIH, abducens paresis, bilateral SDH	Surgery with dura patch at level TH1/2, Clinical improvement, no recurrence of SDH and abducens paresis
Pt 4	31	M	SIH	Several sessions with thoracolumbar blood patches, no improvement
Pt 5	53	F	SIH, bilateral SDH	Blood patch C1/2, surgery of SDH, improvement, no recurrence of SDH
Pt 6	27	F	Rhinorrhoea, frontal encephalocele	Coverage of encephalocele, clinical improvement
Pt 7	69	F	Rhinorrhoea after transsphenoidal surgery	Surgery with coverage of the CSF fistula at the scull base
Pt 8	73	M	Persistent headache and back pain after lumbar surgery	Conservative treatment, clinical improvement
Co 1	45	F	None	None
Co 2	38	M	None	None
Co 3	28	F	None	None
Co 4	35	F	None	None
Co 5	29	M	None	None
Co 6	36	F	None	None

Pt patient, *Co* control subject, *M* male, *F* female

position and the evidence of CSF leakage [4]. Symptoms of SIH may recover without intervention [5]. However in some patients symptoms persist even after multiple epidural blood patches and require more targeted epidural injections, infusions or surgical repair [3]. There is growing evidence that spontaneous CSF leakage may be the common underlying problem [3, 5]. In these patients, confirmation and localization of CSF leak become

Table 2 Scan parameters for T1-weighted sequences with different fat suppression techniques

T1-weighted TSE sequence with	SPIR	SPAIR	3D FFE with Proset WATS
Scan time (min:s)	6:39	6:22	5:20
TR (ms)	450–475	538–686	25
TE (ms)	11	11	5.3
TI (ms)	50	98–108	–
Turbo factor	5	5	–
Bandwidth (Hz)	203.7–238.2	203.7–238.2	134.2
Water fat shift (pixel)	0.912–1.067	0.912–1.067	1.619
Slice number	15–25	15–25	50
Slice thickness/gap (mm)	3/0.3	3/0.3	1.4/−0.7 overcontiguous
Matrix	512×256	512×256	256×256
FOV sagittal and coronal	270×270	270×270	–
FOV axial	225×225	225×225	225×225
Nominal voxel size (mm)	0.44×0.44×3	0.44×0.44×3	0.7×0.7×0.7
Fat suppression technique	Spectral presaturation with inversion recovery	Selective presaturation with adiabatic inversion recovery	Water-selective excitation by spectral spatial pulses

SPIR spectral presaturation with inversion recovery, *SPAIR* selective presaturation with adiabatic inversion recovery, *WATS* water-only selection

important. Radionuclide cisternography may help to confirm a doubtful diagnosis of SIH; however, this method is often insufficient to detect the exact site of the CSF leak [6]. Myelography with postmyelographic thin-slice computed tomography of the entire spine is an accurate method to define the location and extent of a CSF leak [6], with the disadvantage of high radiation exposure [7]. MR myelography after intrathecal injection of gadolinium diethylenetriaminepentaacetic acid (Gd-DTPA) is an increasingly used and promising alternative method to localize CSF leakages [7–9].

In all these studies [7–9] MR myelography is based on T1-weighted images. However information about fat saturation techniques is sparse [7–9]. Anyhow the detection of extraneous contrast agent in fat-laden anatomical regions like the epidural and paravertebral regions requires fat suppression techniques. The most prevalent technique to suppress the signal from fat is frequency-selective fat saturation (SPIR). This technique might be disadvantageous in anatomical regions with intrinsic magnetic field heterogeneities. We describe a reproducible artefact at the cervicothoracic junction of MR imaging using spectral presaturation inversion recovery (SPIR) prepulse after intrathecal administration of Gd-DTPA. To be aware of this imaging feature may reduce false positive results and prevent patients with SIH from invasive treatment modalities.

Materials and methods

Subjects

The study presents a case-control series of MR examinations of eight patients and six healthy volunteers. During the period from 2005 to 2008 Gd-DTPA was administered intrathecally in eight patients for diagnostic purposes because a CSF leakage was, despite negative preceding diagnostic modalities, still highly suspected at different locations. Five patients had symptoms of SIH and underwent intrathecal contrast-enhanced (CE) MR myelography of the whole spine. In the fourth patient with a leakage at the thoracolumbar spine (Table 1) the hyperintense signal was for the first time suspected to be an artefact. Therefore the following patients receiving Gd-DTPA intrathecally for diagnostic purposes also underwent CE MR myelography of the whole spine in addition to the region of suspected CSF leakage (in one patient CSF leakage was suspected after lumbar spine surgery and two patients had CSF rhinorrhoea). In all patients MR myelography was performed as the last diagnostic study because other diagnostic modalities were inconclusive concerning the presence and level of CSF leakage. Additionally six asymptomatic control persons were examined without application of Gd-DTPA. All participants provided informed consent for MR examination. All patients gave written consent for the contrast-enhanced MR myelography after they were informed about the off-label use of Gd-DTPA intrathecally administered 24 h before the intervention. The

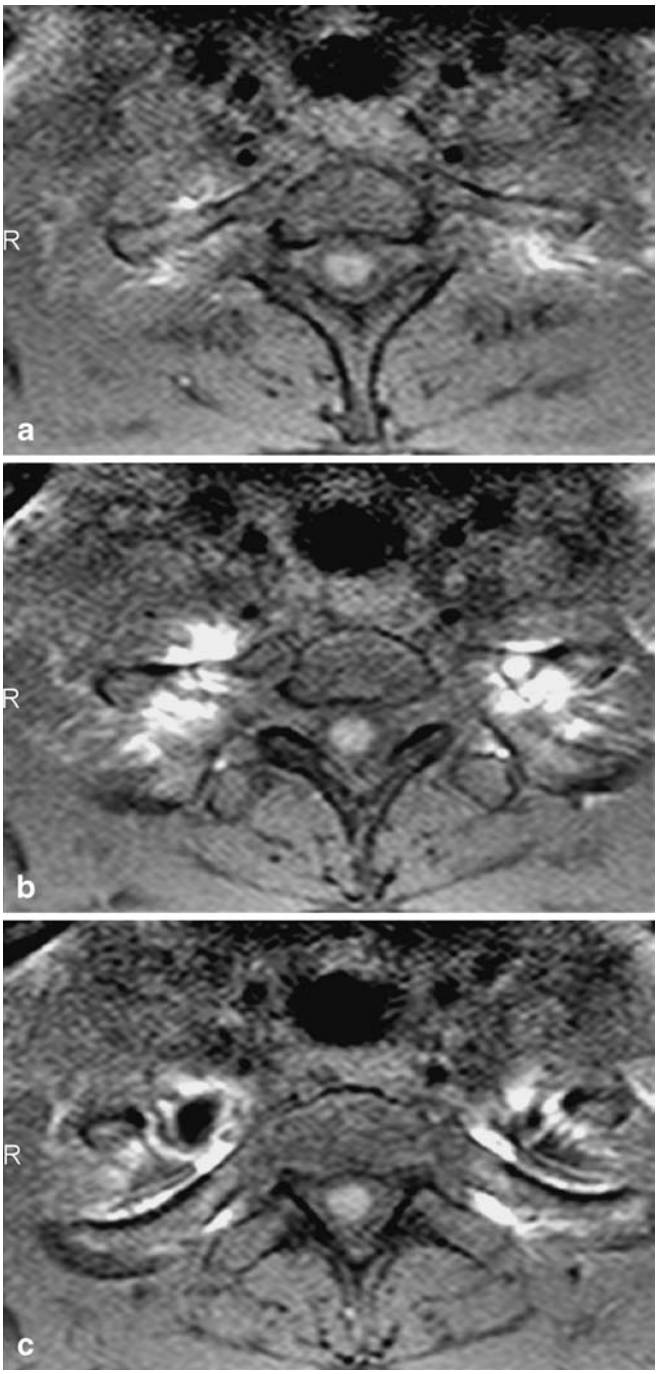

Fig. 1 Axial T1-weighted images with SPIR in a control subject without intrathecal administration of Gd-DTPA. Imaging at level C7/TH1 (**a**) and TH1/TH2 (**b**) showing hyperintense signal in the paraspinal region around the ribs (**a**, **b**) and at the apices of the lung (**c**). There is no hyperintense signal along the nerve roots

responsible physician explained to the patients that the safety of intrathecal application was not tested in prospective clinical trials so far and, even though not reported yet, unwanted effects may occur. Clinical data, patients' symptoms, treatment and follow-up are listed in Table 1 (Table 1).

Technique and MR examination

Lumbar puncture with an atraumatic spinal Sprotte needle (Pajunk Geisingen, Germany, 21-gauge, 0.85 mm) was performed at level L4/5 in all patients. After withdrawal of 4.5 ml CSF, the fluid was mixed with a single volume of Gd-DTPA (0.5 ml, Magnevist; Schering, Berlin, Germany; 469.01 mg of gadopentetate dimeglumine per millilitre) and reinjected into the subarachnoid space under sterile conditions. The needle was removed and the patient told to lie flat. About 10–15 min after injection, with the patient in a supine position, MR examination was performed using a 1.5-T Philips Gyroscan ACS-NT MR system (Best, the Netherlands). In a control group of six healthy volunteers MR was performed with the same protocol without the application of contrast agent. All participants were examined with the same protocol, using T1-weighted turbo spin-echo sequences with a frequency-selective fat saturation pulse (SPIR). The cervical, thoracic and lumbar spine were investigated separately in three orthogonal planes. All levels of neural foramina were examined with axial slices. The suspected anatomical regions were separately investigated further with thin slices, including the skull base in patients with CSF rhinorrhea and the level of lumbar surgery in patient 8. In all sequences a local shim volume was placed at the cervicothoracic junction covering the spine and the adjacent anatomical structures including the paraspinal regions. The size of the shim volume was adapted individually to minimize local field heterogeneities. MR parameters are indicated in Table 2. All patients were observed in the hospital for 24 h after the procedure with clinical and neurological observations including neurological and mental status, subjective complaints, vital signs and headache progression.

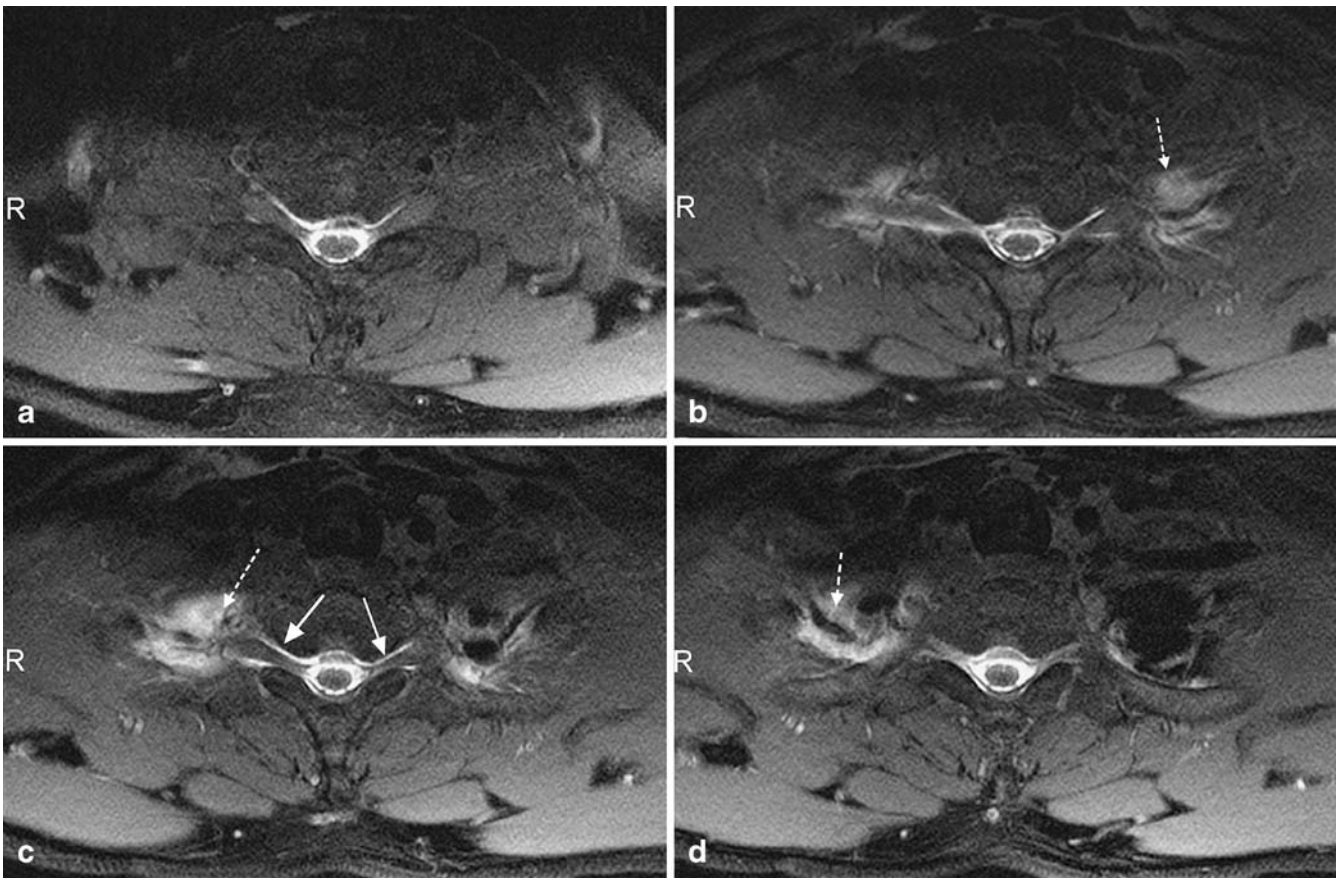

Fig. 2 Axial T1-weighted images with SPIR in a patient with SIH (patient 3) after intrathecal application of diluted 0.5 ml Gd-DTPA showing CSF leakages at level C7/TH1 (**a**–**c**) and TH1/2 (**d**). Images reveal contrast-enhancement in the epidural space and along the dural sheath of the nerve roots on both sides (**c**, *arrows*). This leaking of contrast medium implies the presence of a dural tear. Further bright signal at the apices of the lung (**b**–**d**, *dashed arrow*) might be interpreted as accumulation of contrast agent or as artefact

Evaluation of T1-weighted MR images

Two experienced neuroradiologists reviewed all images. The following imaging features were classified:

1. Presence of bilateral paraspinal hyperintense signal at the level TH1/2
2. Hyperintensity around the nerve roots
3. Hyperintensity in the epidural space

Further evaluation of the artefact

The cause of the reproducible hyperintense signal at the apex of the lung was further analysed with MR spectroscopy and other fat suppression techniques.

MR spectroscopic measurement

To analyse the effect of magnetic field heterogeneity on the chemical shift of water and lipid signals at the apex of the lung MR spectroscopy was performed in three of the six healthy controls. A 2D ^{1}H-MR spectroscopic imaging (^{1}H-MRSI) protocol was performed with and without lipid suppression by frequency-selective pre-saturation at 1.3 ppm. Other parameters were 16×16 matrix, 200×200 mm^2, point-resolved spectroscopy (PRESS) with TR/TE (ms/ms) of 1,320/30, circular phase encoding scheme. The transversal slice was positioned at the apex of the lung (see Fig. 4). Shim procedure was applied using fast map shim algorithm implemented on the MR system; the shim volume covered the PRESS volume.

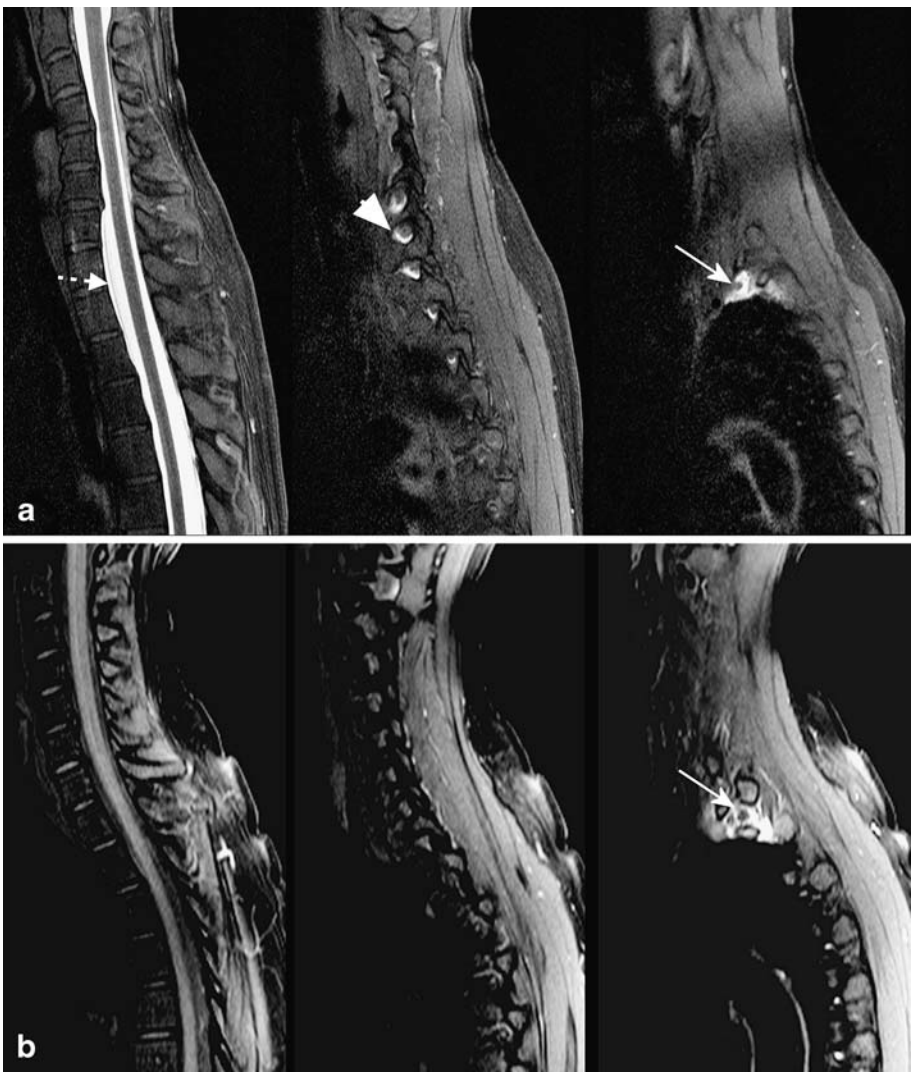

Fig. 3 Sagittal T1-weighted image with SPIR from a patient 2 after intrathecal application of diluted 0.5 ml Gd-DTPA (**a**) showing intradural contrast collection, high signal at the apices of the lung (*arrow*), intraforaminal enhancement along the nerve roots (*arrow head*) and small enhancement of the ventral epidural space (*dashed arrow*). In the control subject only the hyperintense signal at the apices of the lung (*arrow*) is seen (**b**). The relatively high signal of the spinal canal and intervertebral discs in spite of T1 weighting (**b**) is due to their high density of water protons, while protons from fat are suppressed

SPAIR and selective water excitation technique

Spectral attenuation with inversion recovery (SPAIR) and 3D fast field echo (FFE) with a water-only selection pulse (WATS) were used to evaluate sensitivity to the artefact at the apex of the lung. Both sequences are characterized by a lower sensitivity to RF field heterogeneities. Measurements for each method were performed in a control subject without intrathecal administration of contrast medium.

Results

Evaluation of MR images

1. Presence of bilateral paraspinal hyperintense signal at the level TH1/2 in the T1-weighted images with SPIR: All patients and all controls showed hyperintense signal at the apex of the lung. The hyperintense signal was seen in all three orthogonal planes (Figs. 1, 2 and 3).
2. Contrast enhancement around the nerve roots: The contrast enhancement around the nerve roots was absent in all controls (Figs. 1 and 3) and in patients with CSF rhinorrhea. Furthermore, the patient with postoperative symptoms after surgery of lumbar stenosis showed no periradicular contrast enhancement at any level of the whole spine. In the five patients with SIH, three patients showed enhancement around the nerve roots at the cervicothoracic level (Figs. 2 and 3) and one patient at level C1/2. One patient showed enhancement around the nerve roots of the thoracolumbar spine.
3. Accumulation of contrast agent in the epidural space: Accumulation of contrast agent in the ventral epidural space was found in three patients with symptoms of SIH (Figs. 2 and 3). Any enhancement of the epidural space was absent in two of the patients with symptoms of SIH, in all controls and in the patient with CSF rhinorrhea.

Results are summarized in Table 3.

MR spectroscopic measurement

Results of the MR spectroscopic measurement are presented in Fig. 4. The anatomical reference image shows the region of interest. Spectra from blue marked voxel are shown in the graph below. The left panel depicts data obtained without lipid suppression going from the spinal canal in the centre to lateral with the bottom spectrum obtained from a volume in the artefact. The upper spectrum shows the water signal from the spinal canal at 4.7 ppm and a lipid signal at 1.4 ppm. In the artefact, signals were shifted and broadened. The right panel indicates efficient lipid suppression in the spinal canal while in the artefact lipid suppression had no effect.

SPAIR and selective water excitation technique

The subcutaneous fat suppression was more homogenous in the images acquired using T1-weighted sequences with SPAIR. However the artefact at the apex of the lung was still present. In the T1-weighted 3D FFE sequence with the water-selective excitation pulse (WATS) no hyperintensities of fat signal were seen in the critical area at the apex of the lung (Fig. 5).

Table 3 Summary of the MR study results

Participant	GD	Cervicothoracic MR findings (apex of the lung)	Other MR findings
Pt 1	Yes	Bilateral paraspinal hyperintense signal TH1/2	Bilateral enhancement along nerve roots at C7/TH1 and TH1/2 supine position
Pt 2	Yes	Bilateral paraspinal hyperintense signal TH1/2	Bilateral enhancement along nerve roots at C6/7, C7/TH1, TH1/2, TH2/3 right; small epidural GD-DTPA collection
Pt 3	Yes	Bilateral paraspinal hyperintense signal TH1/2	Bilateral enhancement along nerve roots at C7/TH1 and TH1/2; small epidural GD-DTPA collection
Pt 4	Yes	Bilateral paraspinal hyperintense signal TH1/2	Thoracic epidural GD-DTPA collection, small enhancement along nerve roots TH11/12, TH12/L1, L1/2
Pt 5	Yes	Bilateral paraspinal hyperintense signal TH1/2	Cervical epidural GD-DTPA collection, large enhancement C1/2 in the nuchal tissue
Pt 6	Yes	Bilateral paraspinal hyperintense signal TH1/2	Enhancement in ethmoidal cells
Pt 7	Yes	Bilateral paraspinal hyperintense signal TH1/2	Enhancement in sphenoid sinus
Pt 8	Yes	Bilateral paraspinal hyperintense signal TH1/2	None
Co 1–6	No	Bilateral paraspinal hyperintense signal TH1/2	None

GD GD-DTPA, administered intrathecally (yes/no)

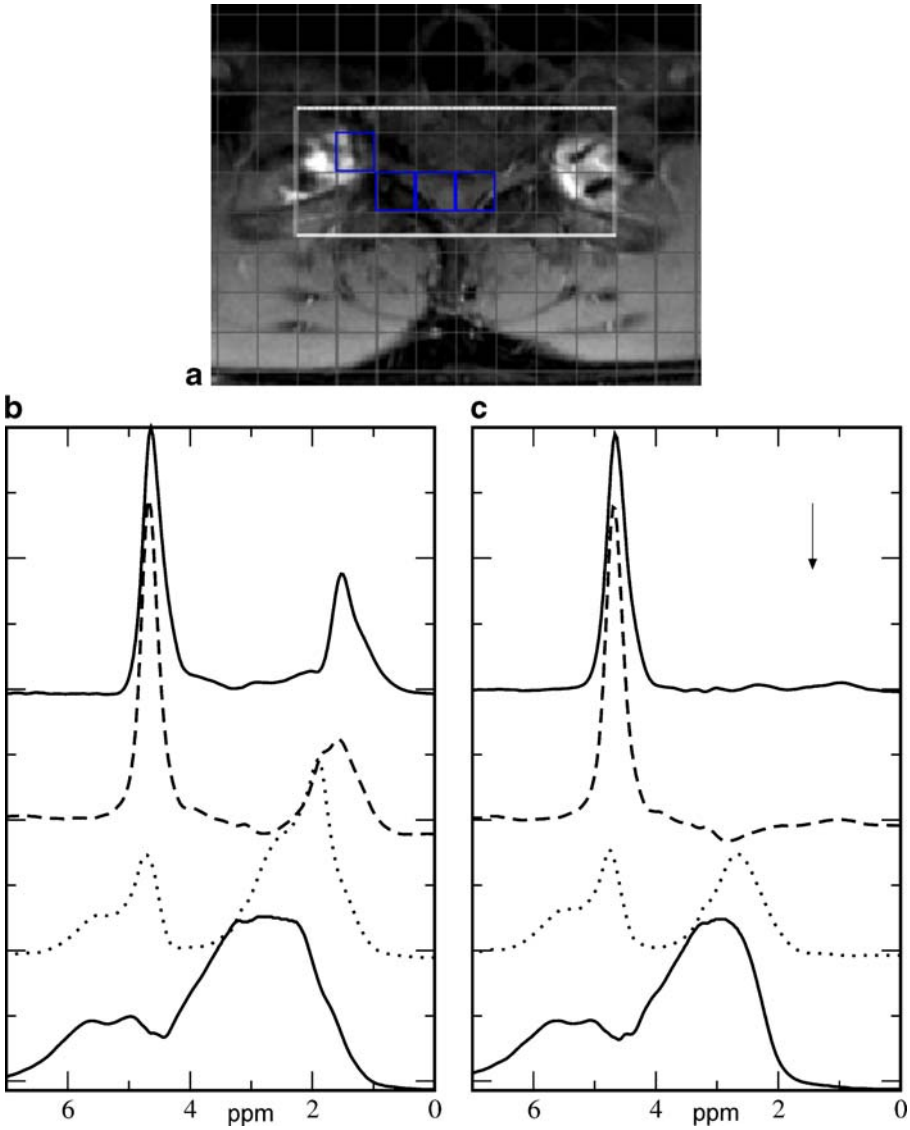

Fig. 4 2D spectroscopic imaging of a transversal slice including the apex of the lung. The reference image (**a**) shows the region of interest (*white square*) selected by the PRESS sequence and marked voxels for spectra analysis shown in **b** and **c**. *Upper* spectra depict data from the spinal canal, and *lower* spectra show data from the lateral voxels going to the artefact at the apex of the lung (*lowest spectra*). **b** Data obtained without lipid suppression. **c** Data acquired with lipid suppression pulse at the frequency position shown by the *arrow*

Discussion

Enhancement of the CSF based on intrathecal application of contrast agent is the most reliable method to detect and to prove CSF leakages. MR myelography after intrathecal administration of Gd-DTPA is an alternative method to CT myelography [10] without ionizing radiation exposure. Apart from detecting CSF leakage in the skull base [11–16], MR myelography with or without intrathecal administration of contrast agent [17] gains increasing importance to detect CSF leakages in patients with SIH [7, 9]. The safety of intrathecal application of Gd-DTPA has been evaluated in several studies [8, 18–19].

Our series from healthy volunteers and patients indicate that CE MR myelography using T1-weighted images with SPIR shows broad hyperintense signals at the apices of the lung, appearing with and without application of Gd-DTPA in all cases. The knowledge of this phenomenon is crucial because it may imitate Gd-DTPA accumulation into the paraspinal tissue. The present imaging pitfall at the apex of the lung was not mentioned so far and clearly has to be classified as an artefact. The location of this artefact is challenging considering that leakages were often found at the cervicothoracic junctions, complicating the differentiation between contrast effusion and artefact (Fig. 1 in [7]) [3].

This artefact shows hyperintense signal at the fat–air interface around the apex of the lung independent from the image planes. Previously it has been demonstrated that fat–air interfaces can cause local failure of fat saturation [20–23]. In fat, the hydrogen nuclei in the $-CH_3$ residue experience some shielding from the evenly shared electron clouds, whereas in the water molecule (H_2O) the strongly electronegative oxygen atom deshields the hydrogen nuclei. Thus hydrogen in fat

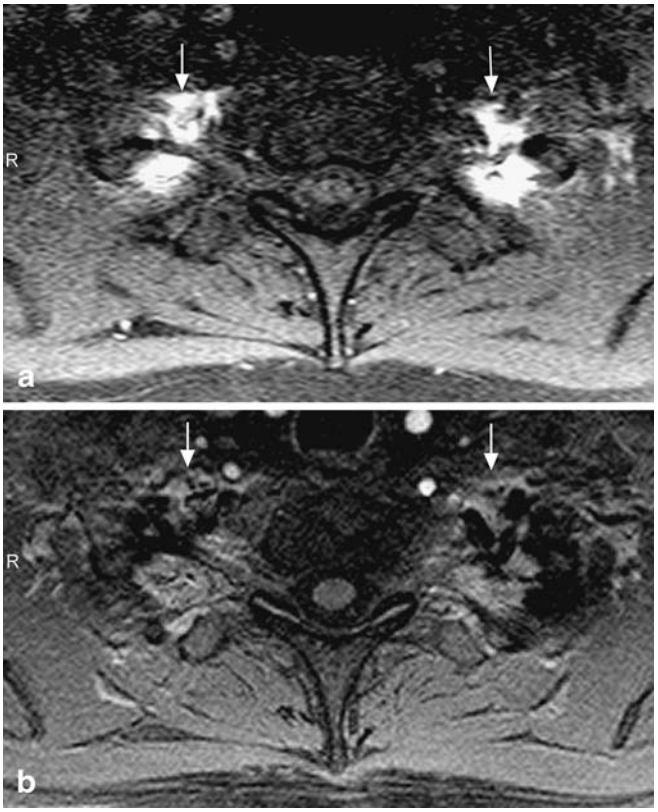

Fig. 5 Axial T1-weighted sequence with SPIR (**a**) compared with the T1-weighted 3D FFE sequence with Proset WATS (**b**) shows a complete suppression of the hyperintense signal (*arrows*) at the apex of the lung in the water excitation technique (**b**)

experiences a lower magnetic field than the water hydrogen resulting in a frequency shift between lipid and water (see Fig. 4b, upper spectrum). SPIR takes advantage of the difference in resonance frequency. A 90° RF pulse, tuned to the resonance frequency of fat, is applied flipping the bulk magnetic vector from fat into the transverse plane. Spoiler gradients are then applied to destroy the phase coherence of the signal. After this saturation routine the imaging sequence follows immediately and the images will only show signal from the remaining water nuclei. The saturation pulse only works if the frequencies of the pulse coincide with the resonance frequency of fat.

Magnetic susceptibility differences at the air–tissue interface at the apex of the lung distort the homogeneity of the static magnetic field. The resulting heterogeneity induces shifts and broadening of the local resonance frequencies causing a mismatch between the frequency of the saturation pulse and the actual frequency of the lipid signal and consequently failure of the lipid suppression. This is demonstrated in the short-echo spectra from MRSI presented in Fig. 4. Taking the spinal canal as starting point and going laterally to the artefact, the signal shifts to the left while concomitant increase in line broadening indicates a significant drop in the field homogeneity. Spectral lipid suppression by frequency-selective pulses was very efficient in the spinal canal, but had no effect at the apex of the lung. The fat suppression failure at the sharp air–fat interface along the main magnetic field direction was also shown by Anzai et al. who used a phantom of the three compartments air, fat and water [20]. Higher field strengths increase these susceptibility effects so that a brighter artefact should be expected at 3 T. In the case of a perfectly homogeneous field, fat suppression should be improved at higher field strengths owing to the increased chemical shift between fat and water. In the presence of field inhomogeneities this improvement is compromised because susceptibility-induced frequency shifts scale exactly with the water–fat shift, so potentially the artefacts described in this paper will remain similar at 3 T. The effect of field strength on this type of artefact cannot be predicted in detail without further experiments. Bandwidth and frequency offset of the T1w sequence with SPIR could be optimized to the individual chemical shift of the lipid signal close to the lung apices. This procedure would require spectroscopic evaluation of this chemical shift. Again this strategy is time consuming and requires operator's expertise. Furthermore SPAIR represents another spectral fat saturation technique which gains clinical importance. In contrast to SPIR adiabatic (amplitude and frequency modulated) RF pulses as well as 180° inversion pulses (in contrast to ca. 120° pulses for SPIR) are implemented which cause less sensitivity to RF field inhomogeneities [24]. We could show that this sequence also showed the hyperintense signal at the apex of the lung. Thus this technique does not prevent the artefact, because it is less sensitive to B_1 only, but not to B_0 field heterogeneities.

This problem raises questions regarding other fat suppression techniques. Difference images of T1w images prior and post intrathecal administration of contrast agent would subtract the artefact. However this procedure is not feasible for clinical use, because it requires the completely exact repositioning of the patient before and after lumbar puncture.

Short TI inversion recovery (STIR) represents an alternative fat suppression method which nulls lipid signals based on the T1 value. This method provides uniform fat suppression independent of magnetic field inhomogeneities. However, STIR is not a reliable method for displaying Gd contrast because the contrast agent and fat have similar T1 values. Thus the signal of Gd contrast can also be nulled in STIR sequences [25].

A promising new technique of fat suppression performs water excitation by means of a spectral spatial pulse [26]. These section-selective composite pulses are timed with the "opposed phase" to excite the water signal, while lipid spins are left in equilibrium, thereby producing no signal [27]. The frequency of the spectral spatial pulse is modified accordingly during the scan. This water-selective excitation technique (WATS) pro-

vides improved fat suppression over conventional prepulses because they are less sensitive to magnetic field inhomogeneities [27, 28]. This technique revealed promising results in enhanced MR imaging of the breast and musculoskeletal imaging [29, 30]. The example of the normal subject also showed promising results, so that further investigation should be performed to evaluate this technique for CE-MR myelography.

Limitation of the study

The study presents a case-control evaluation of diagnostic contrast-enhanced MR myelographic examinations in a limited number of patients ($n=8$). This analysis yielded an artefact, which was further investigated in healthy subjects with the same and with complementary MR modalities. The other fat suppression MR methods were performed in one subject without intrathecal administration of Gd-DTPA. Therefore the results of these investigations including the improved fat suppression of the WATS technique should be considered as preliminary results. Furthermore, there is some evidence that contrast collection in the epidural space and/or contrast passage along the nerve roots might be a reliable sign of CSF leakage caused by a tear of intraspinal dura and/or a tear of the radicular dural sheath. The validation of this sign, its differentiation from physiological CSF reabsorption [31, 32] as well as the evaluation of other fat suppression techniques were beyond the scope of this work and should be proved prospectively in a larger patient cohort.

Conclusion

The detection of CSF leakages with contrast-enhanced MR myelography is a sensitive method which, however, may result in false positive results using frequency-selective fat suppressing techniques. Highly reproducible hyperintense signal at the apex of the lungs in MR images using spectral fat saturation may mimic contrast leakage into paraspinal tissue and must be regarded as an artefact. Alternative spatial and spectral selective water excitation techniques as well as contrast tracking along nerve roots and/or contrast collection in the epidural space should be considered to avoid false diagnosis of CSF leakage.

References

1. Schaltenbrand G (1938) Neuere Anschauungen zur Pathophysiologie der Liquorzirkulation. Zentralblatt für Neurochirurgie 5:290–300
2. Schaltenbrand G (1953) Normal and pathological physiology of the cerebrospinal fluid circulation. Lancet 1:805–808
3. Schievink WI (2006) Spontaneous spinal cerebrospinal fluid leaks and intracranial hypotension. JAMA 295:2286–2966
4. Rando TA, Fishman RA (1992) Spontaneous intracranial hypotension: report of two cases and review of the literature. Neurology 42:481–487
5. Mokri B, Krueger BR, Miller GM et al (1991) Meningeal gadolinium enhancement in low-pressure headaches. Ann Neurol 30:294–295
6. Schievink WI, Meyer FB, Atkinson JLD et al (1996) Spontaneous spinal cerebrospinal fluid leaks and intracranial hypotension. J Neurosurg 84:598–605
7. Albayram S, Kilic F, Ozer H et al (2008) Gadolinium-enhanced MR cisternography to evaluate dural leaks in intracranial hypotension syndrome. AJNR Am J Neuroradiol 29:116–121
8. Tali ET, Ercan N, Krumina G et al (2002) Intrathecal gadolinium (gadopentetate dimeglumine) enhanced magnetic resonance myelography and cisternography: results of a multicenter study. Invest Radiol 37:152–159
9. Kraemer N, Berlis A, Schumacher M (2005) Intrathecal gadolinium-enhanced MR myelography showing multiple dural leakages in a patient with Marfan syndrome. AJR Am J Roentgenol 185:92–94
10. Schievink WI, Maya MM, Louy C et al (2008) Diagnostic criteria for spontaneous spinal CSF leaks and intracranial hypotension. AJNR Am J Neuroradiol 29:853–856
11. Siebner HR, Grafin von Einsiedel H, Conrad B (1997) Magnetic resonance ventriculography with gadolinium DTPA: report of two cases. Neuroradiology 39:418–422
12. Zeng Q, Xiong L, Jinkins JR et al (1999) Intrathecal gadolinium-enhanced MR myelography and cisternography: a pilot study in human patients. AJR Am J Roentgenol 173:1109–1115
13. Wenzel R, Leppien A (2000) Gadolinium-myelocisternography for cerebrospinal fluid rhinorrhoea. Neuroradiology 42:874–880
14. Jinkins JR, Rudwan M, Krumina G et al (2002) Intrathecal gadolinium-enhanced MR cisternography in the evaluation of clinically suspected cerebrospinal fluid rhinorrhea in humans: early experience. Radiology 222:555–559
15. Reiche W, Komenda Y, Schick B et al (2002) MR cisternography after intrathecal Gd-DTPA application. Eur Radiol 12:2943–2949
16. Aydin K, Guven K, Sencer S et al (2004) MRI cisternography with gadolinium-containing contrast medium: its role, advantages and limitations in the investigation of rhinorrhoea. Neuroradiology 46:75–80
17. Tomoda Y, Korogi Y, Aoki T et al (2008) Detection of cerebrospinal fluid leakage: initial experience with three-dimensional fast spin-echo magnetic resonance myelography. Acta Radiol 49:197–203
18. Ray DE, Cavanagh JB, Nolan CC et al (1996) Neurotoxic effects of gadopentetate dimeglumine: behavioral disturbance and morphology after intracerebroventricular injection in rats. AJNR Am J Neuroradiol 17:365–373

19. Skalpe IO (1998) Is it dangerous to inject MR contrast media into the subarachnoid space? Acta Radiol 39:100
20. Anzai Y, Lufkin RB, Jabour BA et al (1992) Fat-suppression failure artifacts simulating pathology on frequency-selective fat-suppression MR images of the head and neck. AJNR Am J Neuroradiol 13:879–884
21. Borges AR, Lufkin RB, Huang AY et al (1997) Frequency-selective fat suppression MR imaging. Localized asymmetric failure of fat suppression mimicking orbital disease. J Neuroophthalmol 17:12–17
22. Delfaut EM, Beltran J, Johnson G et al (1999) Fat suppression in MR imaging: techniques and pitfalls. Radiographics 19:373–382
23. Yoshimitsu K, Varma DG, Jackson EF (1995) Unsuppressed fat in the right anterior diaphragmatic region on fat-suppressed T2-weighted fast spin-echo MR images. J Magn Reson Imaging 5:145–149
24. Mürtz P, Krautmacher C, Träber F et al (2007) Diffusion-weighted whole-body MR imaging with background body signal suppression: a feasibility study at 3.0 Tesla. Eur Radiol 17:3031–3037
25. Krinsky G, Rofsky NM, Weinreb JC (1996) Nonspecificity of short inversion time inversion recovery (STIR) as a technique of fat suppression: pitfalls in image interpretation. AJR Am J Roentgenol 166:523–526
26. Meyer CH, Pauly JM, Macovski A, Nishimura DG (1990) Simultaneous spatial and spectral selective excitation. Magn Reson Med 15:287–304
27. Schick F, Forster J, Machann J, Huppert P et al (1997) Highly selective water and fat imaging applying multi-slice sequences without sensitivity to B1 field inhomogeneities. Magn Reson Med 38:269–274
28. Zur Y (2000) Design of improved spectral-spatial pulses for routine clinical use. Magn Reson Med 43:410–420
29. Niitsu M, Tohno E, Itai Y (2003) Fat suppression strategies in enhanced MR imaging of the breast: comparison of SPIR and water excitation sequences. J Magn Reson Imaging 18:310–314
30. Hauger O, Dumont E, Chateil JF et al (2002) Water excitation as an alternative to fat saturation in MR imaging: preliminary results in musculoskeletal imaging. Radiology 224:657–663
31. Zenker W, Bankoul S, Braun JS (1994) Morphological indications for considerable diffuse reabsorption of cerebrospinal fluid in spinal meninges particularly in the areas of meningeal funnels. An electronmicroscopical study including tracing experiments in rats. Anat Embryol (Berl) 189:243–258
32. Bozanovic-Sosic R, Mollanji R, Johnston MG (2001) Spinal and cranial contributions to total cerebrospinal fluid transport. Am J Physiol Regul Integr Comp Physiol 281:R909–R916